Research Journal of Applied Sciences, Engineering and Technology 7(13): 2714-2723, 2014
DOI:10.19026/rjaset.7.591
ISSN: 2040-7459; e-ISSN: 2040-7467

Submitted: September 09, 2013 Accepted: October 07, 2013 Published: April 05, 2014

Research Article

Design and Implementation of a Power Converter to Process Renewable Energy for Step-down Voltage Applications

Chih-Lung Shen and Yu-Sheng Shen
Department of Electronic Engineering, National Kaohsiung First University of Science and Technology, Yanchao, Kaohsiung 824, Taiwan

Abstract: In this study a power converter to process renewable energy is proposed, which can not only process solar energy but deal with wind power. The proposed converter is derived from two series modified forwards to step down voltage for charger system or dc distribution application, so as called Modified-Forward Dual-Input Converter (MFDIC). The MFDIC mainly contains an upper Modified Forward (MF), a lower MF, a common output inductor and a DSP-based system controller. The upper and lower MFs can operate individually or simultaneously to accommodate the variation of atmospheric conditions. Since the MFDIC can process renewable power with interleaved operation, the ripple of output current is suppressed significantly and thus better performance is achieved. In the MFDIC only a common output inductor is needed, instead of two separated inductors, so that the volume of the converter is reduced significantly. To draw maximum power from PV panel and wind turbine, perturb-and-observe method is adopted to achieve the feature of Maximum Power Point Tracking (MPPT). The MFDIC is constructed, designed, analyzed, simulated and tested. Simulations and practical measurements have demonstrated the validity and the feasibility of the proposed dual-input converter.

Keywords: Modified forward converter, solar energy, step-down voltage, wind power

INTRODUCTION

With rapid development of industry and commerce, requirement for electricity has been growing dramatically. Conventionally, electric power is mainly generated from fossil fuels. However, this kind of energy resources is highly limited and will exhaust in the near future. Therefore, adopting renewable and clean energy resources to replace fossil fuels for electric power generation is a research of great urgency. Among renewable resources, solar energy and wind power attract a great deal of interest owing to their easy acquirement.

In Photovoltaic (PV) or wind power generation system, a power converter is needed to process renewable energy. In literature (Wai and Wang, 2008; Gules *et al*., 2008; Vazquez *et al*., 2008; Lohmeier *et al*., 2011; Shen and Chau, 2012) PV converters are presented while wind power converters are discussed in Yazdani and Iravani (2006) and Ullah and Thiringer (2007). However, these power converters only handle single kind of renewable energy, that is, which cannot deal with multi-input power. Therefore, some researchers propose multi-input converters for solar/wind hybrid power generation system (Sedaghati and Babaei, 2011; Cacciato *et al*., 2008; Fang and Ma, 2010). Even though these multi-input converters can process hybrid renewable energy, two separated converters in series or in parallel are required. A series double-boost converter is presented to process PV power and wind energy simultaneously, in which, as compared with single-boost configuration, power component only imposes one-half of the voltage stress (Solero *et al*., 1996). Because boost-type converter steps up voltage, it is not suitable for low voltage and galvanic isolated applications. Double-input buck-boost converter is capable of processing high-/low-voltage sources (Chen *et al*., 2007); however, this type of configuration is non-isolated electrically. Besides, the output voltage has opposite polarity from the input voltage. Instead of combining renewable energy in electricity, the concept of magnetic flux additivity is proposed for the design of multi-input converter but complicated control low and complex structure are required (Chen *et al*., 2002).

In this study, a Modified-Forward Dual-Input Converter (MFDIC) is proposed, which can deal with PV power and wind energy simultaneously or individually. The converter is composed of two modified series forward converters with a common output filter inductor, which simplifies multi-input structure and lowers cost. Furthermore, the converter

Corresponding Author: Chih-Lung Shen, Department of Electronic Engineering, National Kaohsiung First University of Science and Technology, University Road, Yanchao, Kaohsiung 824, Taiwan, Tel.: +886-7-6011000; Fax: +886-7-6011386

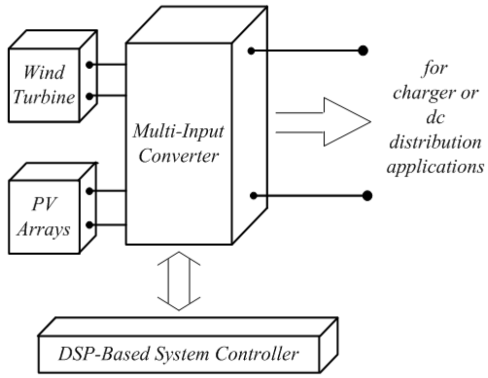

Fig. 1: A block diagram to illustrate a PV-wind power generation system

can draw maximum power from PV arrays and wind turbine by perturb-and-observe method. The system controller of the converter can be implemented in a DSP chip to lower the total number of discrete devices, which reduces the volume of the converter and promotes its reliability. A prototype of the MFDIC is built for demonstration. Key waveforms measured from the prototype are shown in this study to verify the validity and the feasibility of the proposed converter.

METHODOLOGY

System architecture: A block diagram to illustrate a PV-wind power generation system is shown in Fig. 1, which mainly contains a PV panel, a wind turbine, a multi-input converter and a system controller. In order to process PV power and wind-turbine energy, in this study a modified-forward dual-input converter is derived. Figure 2 shows the schematic of the main power circuit of the proposed converter. The MFDIC consists of an upper Modified Forward (MF), a lower MF, a common output filter inductor and a DSP-based system controller. The upper MF processes the electricity of wind energy, while the lower one deals with PV power. Both upper and lower MF s can be operated individually or simultaneously. The system controller can be implemented in a DSP chip to perform power calculations, Maximum Power Point Tracking (MPPT), control signal determination, over-voltage protection, over-current protection and dc-link voltage regulation.

Operation principle of the proposed converter: In Fig. 2, the upper MF and the lower MF can work

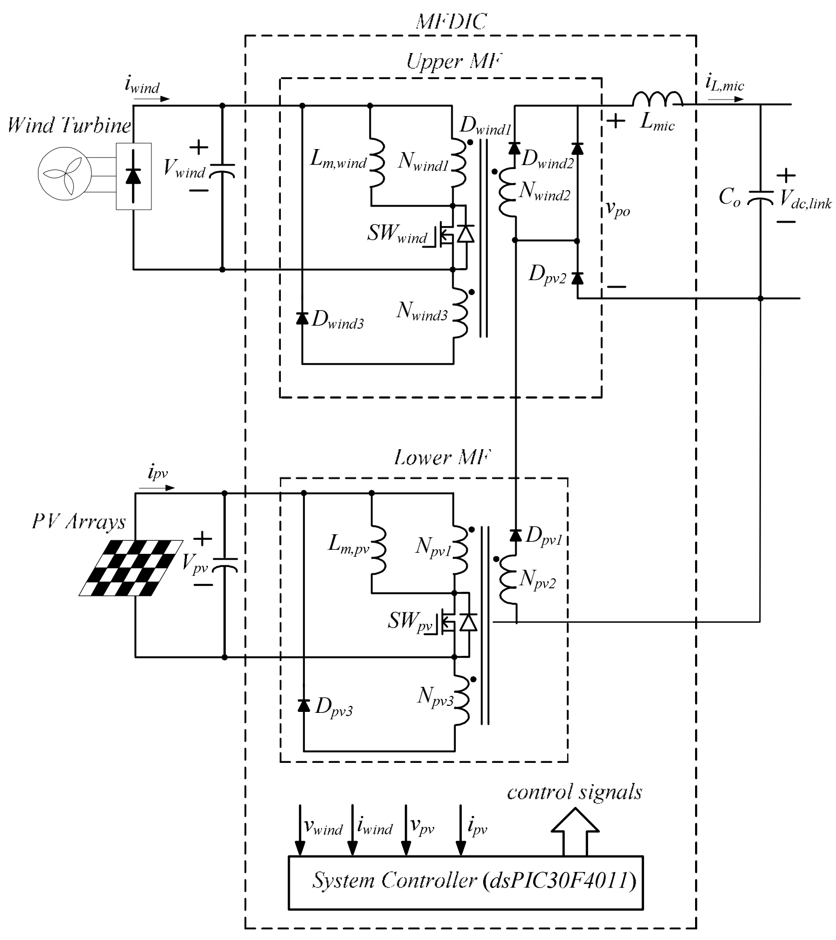

Fig. 2: The configuration of the proposed MFDIC

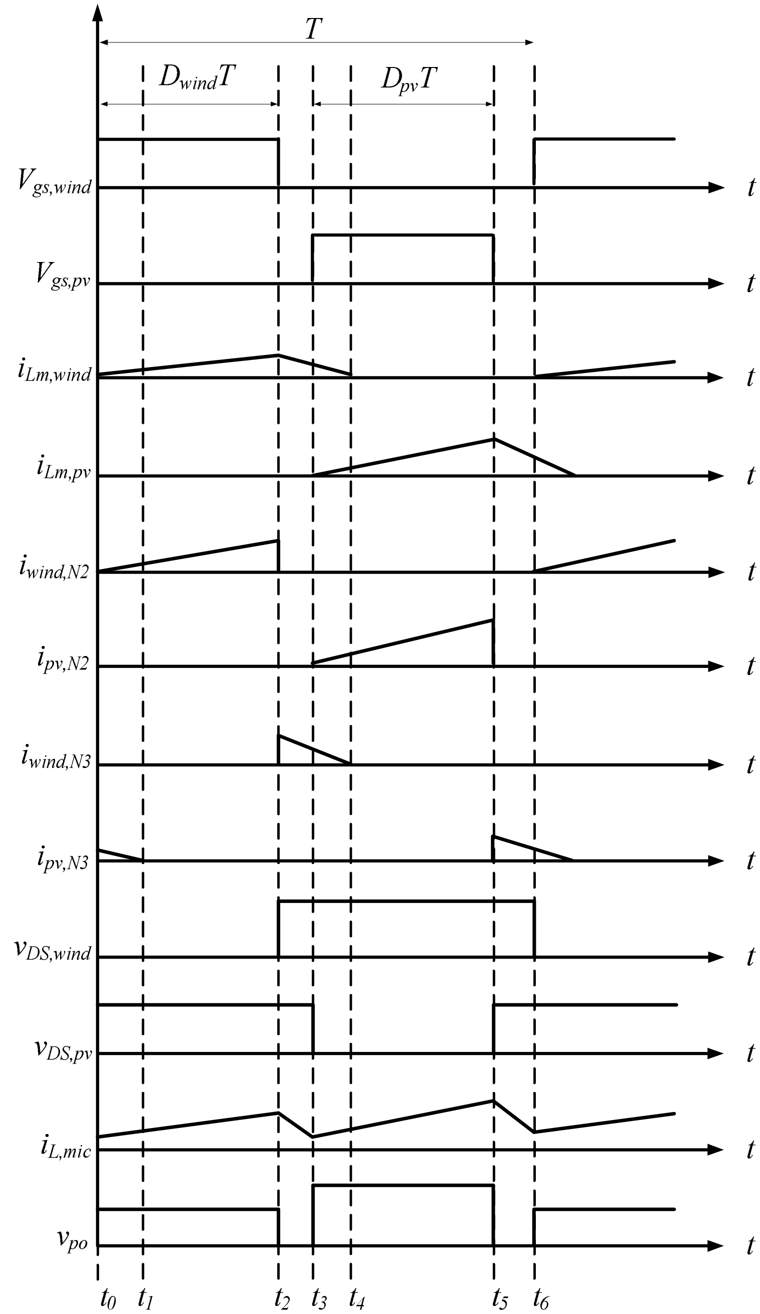

Fig. 3: Control signals and related key waveforms

individually. To achieve better output performance and to lower hardware volume, both modified forwards are designed in interleaved operation and with the same switching frequency. The Fig. 3 shows conceptual control signals and related key waveforms. According to the conduction status of the switches SW_{wind} and SW_{pv}, the operation of the MFDIC over one switching period can mainly be divided into six modes. Corresponding equivalents are presented in Fig. 4. The operation principle is described mode by mode in the followings.

Mode 1 (Fig. 4a, $t_0 \le t < t_1$): This mode begins when SW_{wind} starts conducting at t_0. In this mode, the active switch SW_{pv} is in the off state and the magnetizing inductor of the lower modified forward still discharges energy through the path of N_{pv3}-D_{pv3}-C_{pv}. Wind power is forwarded to output and the output inductor current $i_{L,mic}$ is increasing linearly. As the current of magnetizing-inductor $L_{m,pv}$ drops to zero, this mode ends.

Mode 2 (Fig. 4b, $t_1 \le t < t_2$): During the interval of this mode, SW_{wind} conducts continuously; meanwhile,

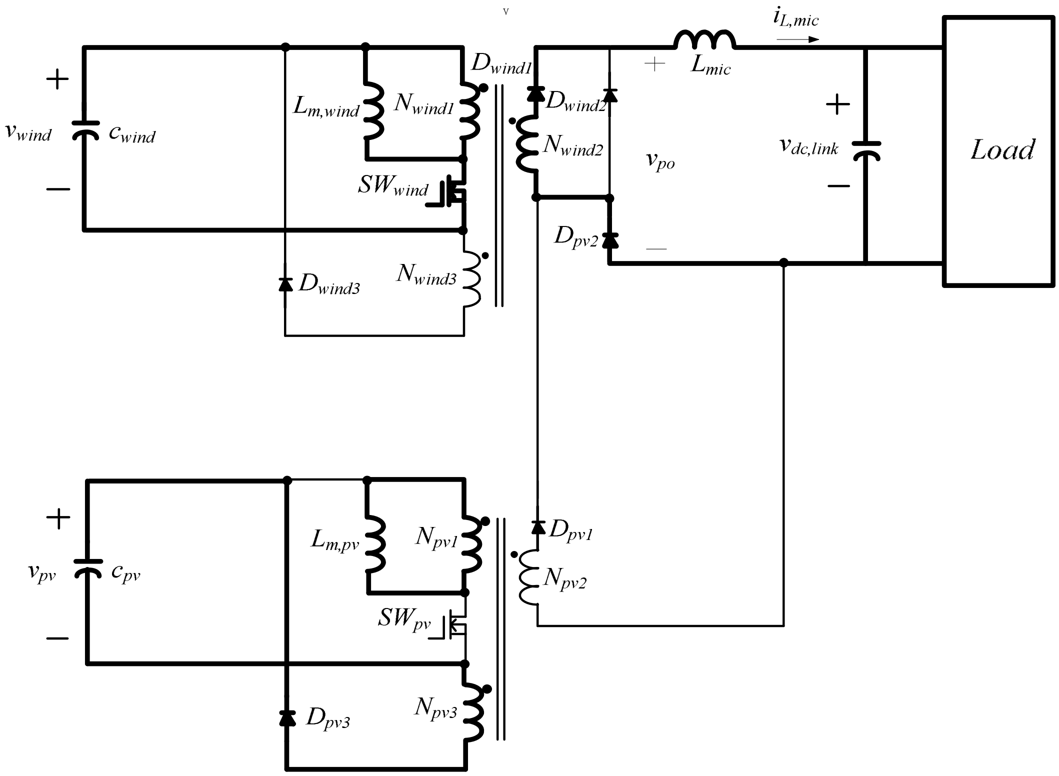

$i_{L,mic}$
L_{mic}
D_{wind1}
D_{wind2}
N_{wind2}
D_{pv2}
v_{po}
$v_{dc,link}$
Load
v_{wind}
c_{wind}
$L_{m,wind}$
N_{wind1}
SW_{wind}
D_{wind3}
N_{wind3}
v_{pv}
c_{pv}
$L_{m,pv}$
N_{pv1}
D_{pv1}
N_{pv2}
SW_{pv}
D_{pv3}
N_{pv3}

(a)

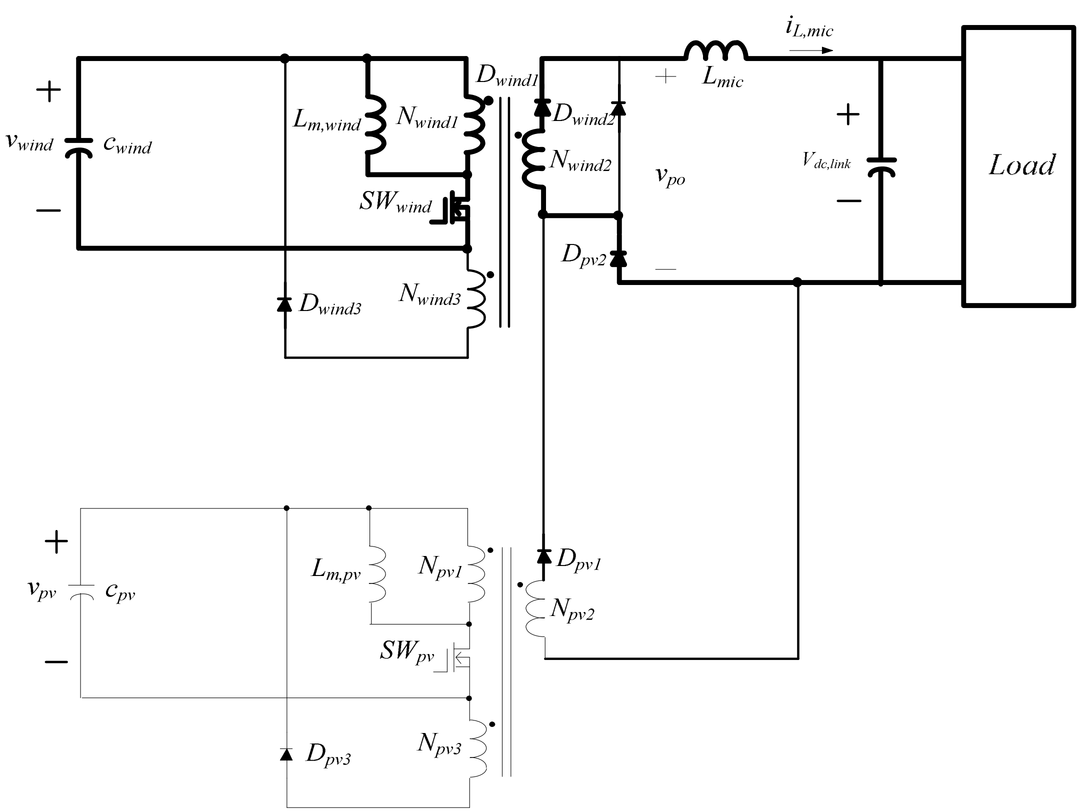

$i_{L,mic}$
L_{mic}
D_{wind1}
D_{wind2}
N_{wind2}
D_{pv2}
v_{po}
$V_{dc,link}$
Load
v_{wind}
c_{wind}
$L_{m,wind}$
N_{wind1}
SW_{wind}
D_{wind3}
N_{wind3}
v_{pv}
c_{pv}
$L_{m,pv}$
N_{pv1}
D_{pv1}
N_{pv2}
SW_{pv}
D_{pv3}
N_{pv3}

(b)

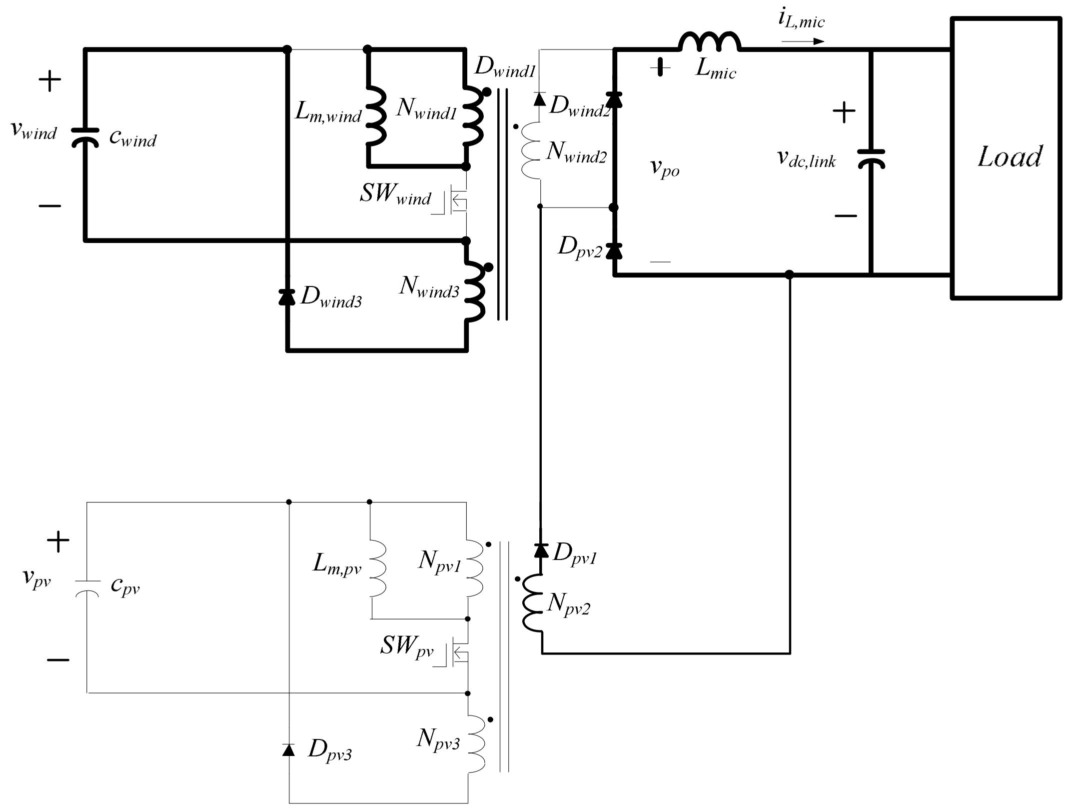
$i_{L,mic}$
L_{mic}
D_{wind1}
D_{wind2}
N_{wind1}
N_{wind2}
N_{wind3}
$L_{m,wind}$
v_{wind}
c_{wind}
SW_{wind}
D_{wind3}
D_{pv2}
v_{po}
$v_{dc,link}$
Load
v_{pv}
c_{pv}
$L_{m,pv}$
N_{pv1}
N_{pv2}
N_{pv3}
D_{pv1}
D_{pv3}
SW_{pv}

(c)

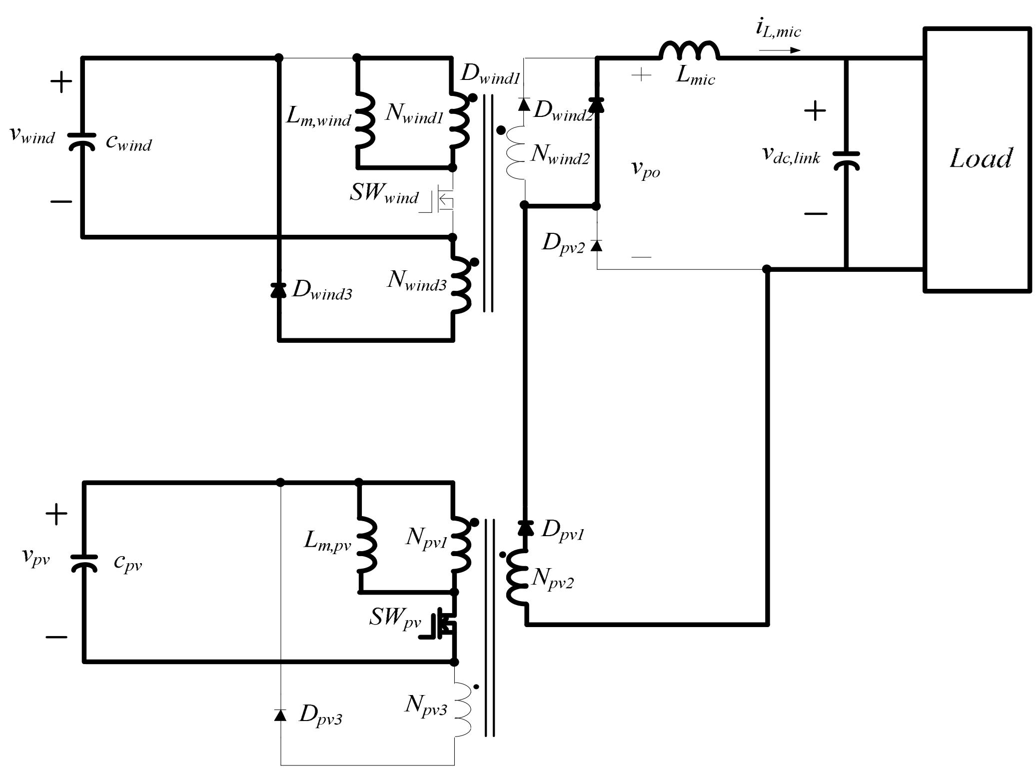
$i_{L,mic}$
L_{mic}
D_{wind1}
D_{wind2}
N_{wind1}
N_{wind2}
N_{wind3}
$L_{m,wind}$
v_{wind}
c_{wind}
SW_{wind}
D_{wind3}
D_{pv2}
v_{po}
$v_{dc,link}$
Load
v_{pv}
c_{pv}
$L_{m,pv}$
N_{pv1}
N_{pv2}
N_{pv3}
D_{pv1}
D_{pv3}
SW_{pv}

(d)

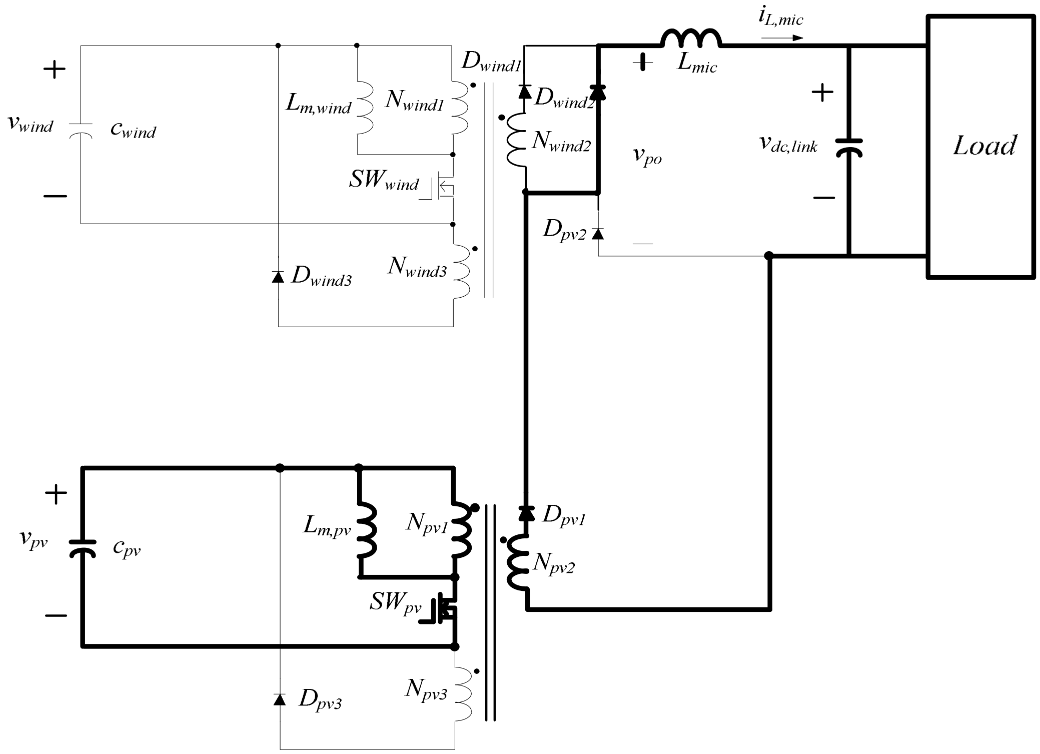

(e)

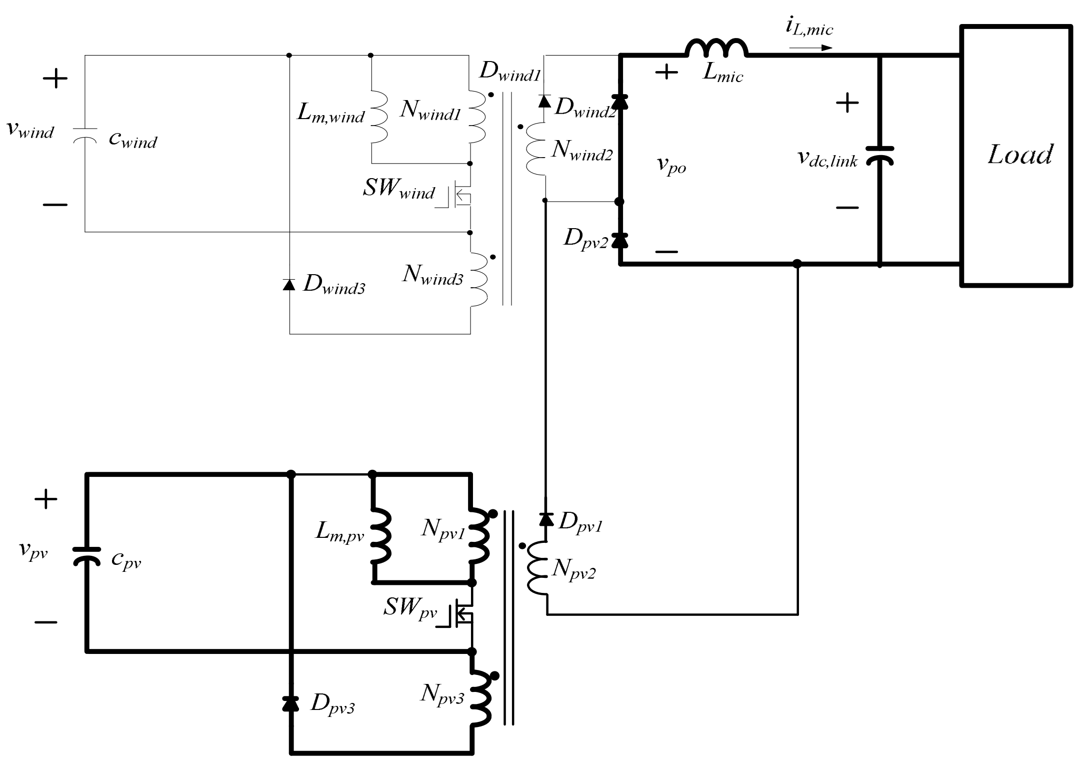

(f)

Fig. 4: Equivalent circuits of the MFDIC corresponding to the six operation modes over one switching cycle, (a) mode 1, (b) mode 2, (c) mode 3, (d) mode 4, (e) mode 5 and (f) mode 6

D_{wind1} and D_{pv2} are on. The current $i_{L,mic}$ keeps increasing and can be represented as:

$$i_{L,mic} = \frac{1}{L_{mic}}(v_{wind} \cdot \frac{N_{wind2}}{N_{wind1}} - v_{dc,link})t + i_{L,mic}(t_0) \quad (1)$$

where,

L_{mic} = The output inductance
v_{wind} = The voltage of wind turbine
$v_{dc,link}$ = The output voltage of the MFMIC

Mode 3 (Fig. 4c, $t_2 \leq t < t_3$): At time t_2, the switch SW_{wind} is turned off and SW_{pv} in the lower modified forward still stays in the off state. The output inductor L_{mic} releases stored energy to the load by the path of L_{mic}-C_o-D_{pv2}-D_{wind2}. Since the voltage v_{po} is equal to the sum of cut-in voltages of D_{wind2} and D_{pv2}. Thus, during this interval the change in the output inductor current can be determined by:

$$\Delta i_{L,mic} = \frac{V_{dc,link} - (V_{r,wind2} + V_{r,pv2})}{L_{mic}} \cdot (\frac{1}{2f_s} - D_{wind}\ T) \quad (2)$$

In which f_s is the switching frequency of the MFDIC, D_{wind} expresses the duty ratio of the upper MF, T denotes switching period and $V_{r,wind2}$ and $V_{r,pv2}$ stand for the cut-in voltages of D_{wind2} and D_{pv2}, respectively. In mode 3, the magnetizing inductor in the upper modified forward discharges via the path of N_{wind3}-D_{wind3}-C_{wind}.

Mode 4 (Fig. 4d, $t_3 \leq t < t_4$): The SW_{pv} is turned on at t_3 and thus PV energy is dealt with by the lower modified forward. The inductor current $i_{L,mic}$ increases linearly. In

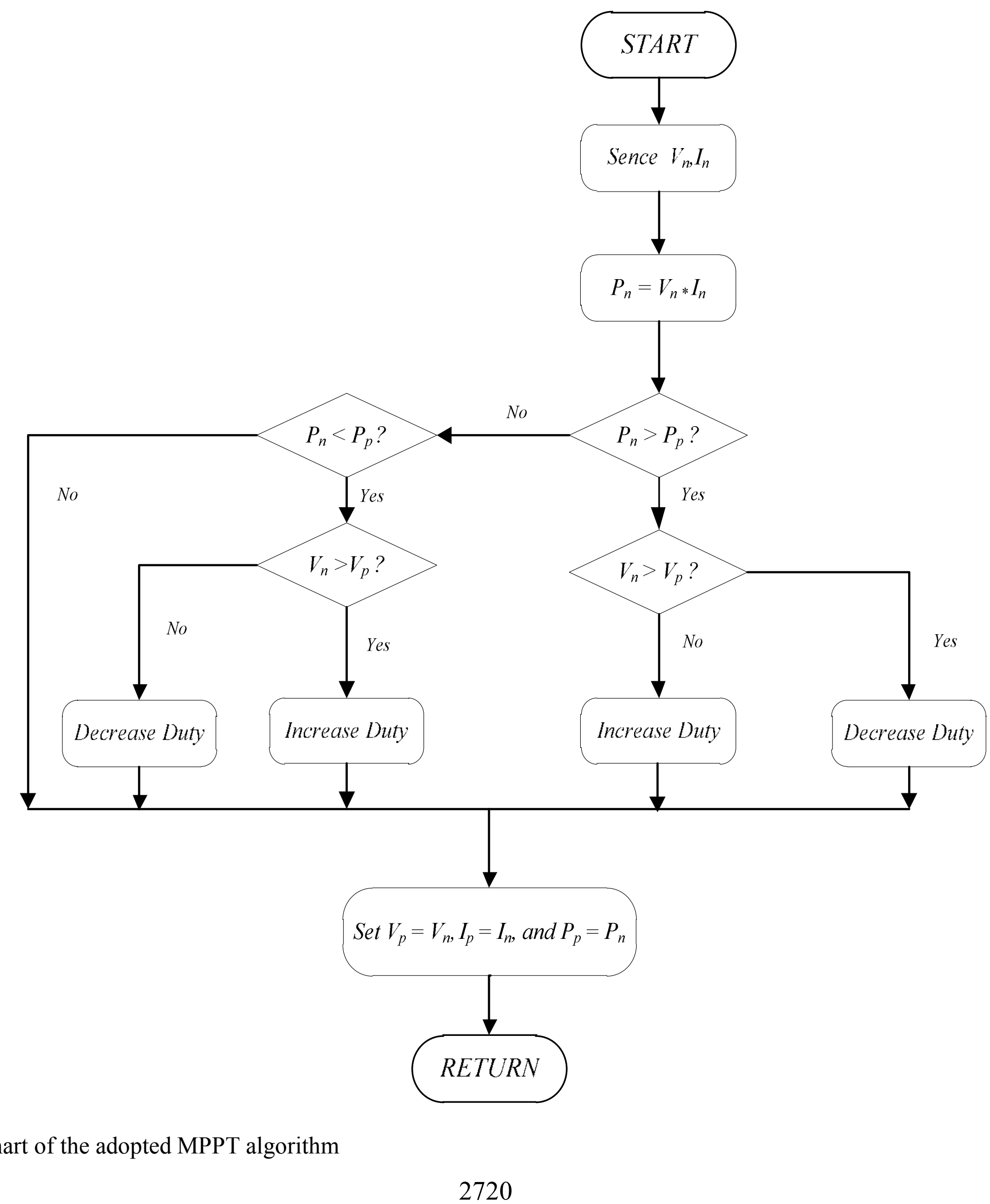

Fig. 5: Flowchart of the adopted MPPT algorithm

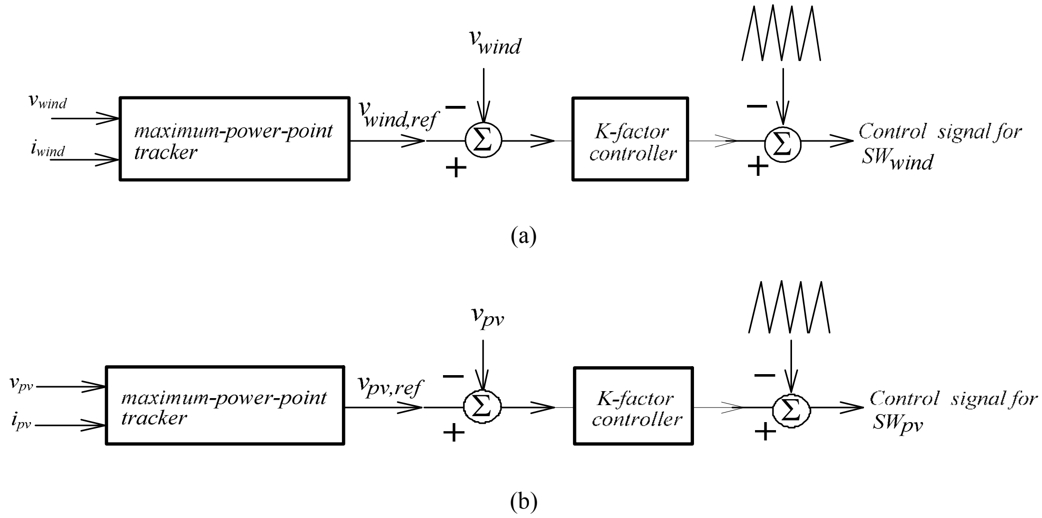

Fig. 6: Simplified control block diagram of the converter, (a) controlling for upper MF, (b) for lower MF

mode 4, inductor $L_{m,wind}$ discharges through N_{wind1}, N_{wind3}, D_{wind3} and C_{wind}. This mode ends at the moment the current flowing through $L_{m,wind}$ equals zero.

Mode 5 (Fig. 4e, $t_4 \le t < t_5$): In this mode, SW_{pv} maintains in the on state and $i_{L,mic}$ increases continuously. Diodes D_{wind2} and D_{pv1} are on but D_{wind3} and D_{pv2} are off. A reversed voltage across D_{pv2} is:

$$v_{D,pv2} = \frac{N_{pv2}}{N_{pv1}} \cdot v_{pv} \tag{3}$$

in which v_{pv} is the terminal voltage of PV arrays.

Mode 6 (Fig. 4f, $t_5 \le t < t_6$): At time t_5, the switch SW_{pv} is turned off and the operation of MFDIC enters into mode 6. The magnetizing inductor $L_{m,pv}$ releases energy to capacitor C_{pv} via N_{pv1}, N_{pv3} and D_{pv3}. Meanwhile, the current $i_{L,mic}$ decreases linearly. A complete switching cycle is terminated at $t = t_6$, at which SW_{wind} is turned on again.

To draw maximum power from PV arrays and wind generator, the perturb-and-observe method is adopted to accomplish MPPT feature, of which flowchart is illustrated in Fig. 5. In addition, a simplified control block diagram is also shown in Fig. 6. According to various atmospheric conditions, the maximum-power-point trackers determine optimal terminal voltages ($v_{wind,ref}$ and $v_{pv,ref}$) for PV arrays and wind turbine so as to draw maximum power from the two renewable generators. Then, the commands are compared with practical voltages. An error is fed to the K-factor controllers for the determination of control signals. The total amount of the converter output power P_o is calculated by:

$$P_o = \left(\frac{N_{wind2} D_{wind} v_{wind}}{N_{wind1}} + \frac{N_{pv2} D_{pv} v_{pv}}{N_{pv1}}\right) \cdot I_{L,mic} \tag{4}$$

where $I_{L,mic}$ stands for the average current of the output inductor.

SIMULATED AND EXPERIMENTAL RESULTS

An MFDIC system is constructed, designed, analyzed, simulated and measured to verify its feasibility and validity. Some important parameters are listed as follows:

- PV arrays: SIEMENS SM55
- PV panel voltage: v_{pv} = 48-54 V (3 units in series)
- Wind turbine voltage: v_{wind} = 36-48 V
- Battery voltage (as a load): 12 V
- Switching frequency: 45 kHz for SW_{wind} and SW_{pv},
- Output inductance L_{mic} = 2 mH
- Output capacitance C_o = 330 μF
- Turns ratio: N_{wind1}: N_{wind2}: N_{wind3} = 60:60:30
- N_{pv1}: N_{pv2}: N_{pv3} = 60:60:30
- Power switches: SPW47N60C3
- Ultrafast diode: 60APU06F

During the interval of PV arrays and wind turbine providing power to load simultaneously, Fig. 7 is the measured control signals and Fig. 8 shows the corresponding output inductor current. It can be seen that the MFDIC drives SW_{pv} and SW_{wind} in interleaving mode. The waveform of v_{po} is also shown in Fig. 9, which affects output inductor current and output power directly. While 100 W PV power supplies the MFDIC and then 250 W wind energy cuts in the generation system, the output power variation is shown

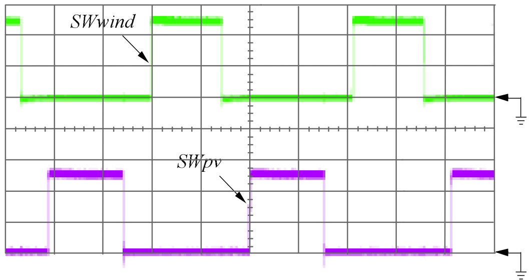

Fig. 7: Measured control signals for SW_{wind} and SW_{pv} (5 V/div; 5 μs/div)

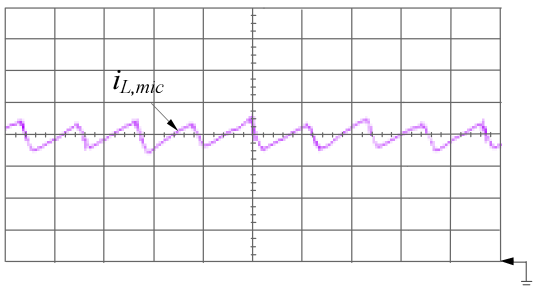

Fig. 8: Measured output inductor current $i_{L,mic}$ (5 A/div; 10 μs/div)

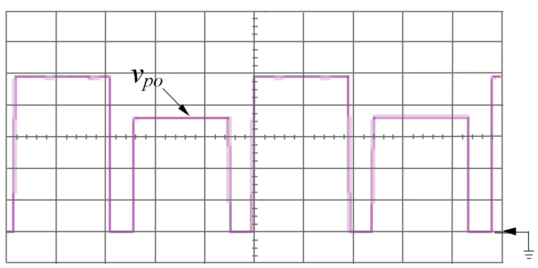

Fig. 9: The waveform of v_{po} (5 V/div; 5 μs/div)

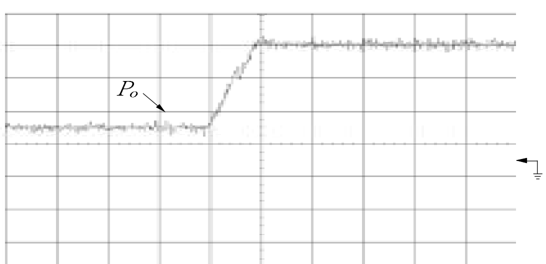

Fig. 10: Output power variation while wind turbine cuts in the MFMIC (100 W/div; 1 s/div)

in Fig. 10. In the case of 180 W wind-turbine energy shunting down from the MFDIC, the variation of the output power is shown in Fig. 11. Provided only PV power is processed and solar varies from intensive irradiation to medium irradiation, the curve of output power is shown in Fig. 12. From Fig. 10 to 12, it has been verified that the proposed MFDIC can deal with

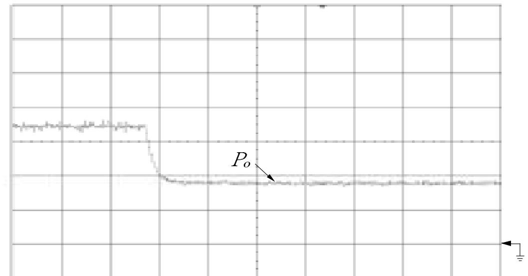

Fig. 11: Output power variation while wind turbine shunts down from the MFDIC (100 W/div; 1 s/div)

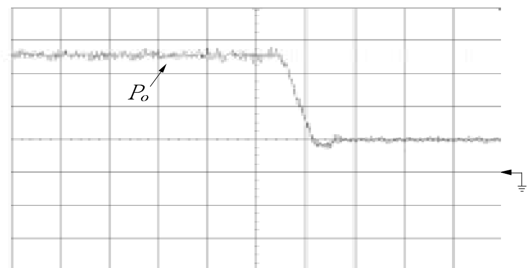

Fig. 12: Power variation of the MFMIC while solar varies from intensive irradiation to medium irradiation (100 W/div; 1 s/div)

renewable power effectively under different atmospheric conditions.

CONCLUSION

This study proposed a modified-forward multi-input converter to deal with renewable energy. The converter is derived from two series forward converters, which is able to process PV power and wind energy simultaneously or individually under various atmospheric conditions. Instead of two separated converters, the proposed MFDIC has lower volume and is cost-effective. In this study, the MFDIC is designed, analyzed and measured. Key waveforms have demonstrated the feasibility of the proposed converter.

REFERENCES

Cacciato, M., A. Consoli, N. Aiello, R. Attanasio, F. Gennaro and G. Macina, 2008. A digitally controlled double stage soft-switching converter for grid-connected photovoltaic applications. Proceedings of the 23rd Annual IEEE Applied Power Electronics Specialists Conference, pp: 141-147.

Chen, Y.M., Y.C. Liu and F.Y. Wu, 2002. Multi-input dc/dc converter based on the multiwinding transformer for renewable energy applications. IEEE T. Ind. Appl., 38(4): 1096-1104.

Chen, Y.M., Y.C. Liu, S.C. Hung and C.S. Cheng, 2007. Multi-input inverter for grid-connected hybrid PV/wind power system. IEEE T. Power Electron., 22(3): 1070-1077.

Fang, Y. and X. Ma, 2010. A novel PV microinverter with coupled inductors and double-boost topology. IEEE T. Power Electron., 25(12): 3139-3147.

Gules, R., J.D.P. Pacheco, H.L. Hey and J. Imhoff, 2008. A maximum power point tracking system with parallel connection for PV stand-alone applications. IEEE T. Ind. Electron., 55: 2674-2683.

Lohmeier, C., J.W. Zeng, Q. Wei, L. Qu and J. Hudgins, 2011. A current-sensorless MPPT quasi-double-boost converter for PV systems. Proceedings of the IEEE Power Electronics Specialists Conference, pp: 1069-1075.

Sedaghati, F. and E. Babaei, 2011. Double input z-source dc-dc converter. Proceedings of the IEEE Power Electronics Specialists Conference, pp: 581-586.

Shen, C.L. and J.S. Chau, 2012. Grid-connection half-bridge PV inverter system for power flow controlling and active power filtering. Int. J. Photoenergy, Article ID 760791, 2012: 8.

Solero, L., F. Caricchi, F. Crescimbini, O. Honorati and F. Mezzetti, 1996. Performance of a 10 kW power electronic interface for combined wind/PV isolated generating systems. Proceedings of the IEEE Power Electronics Specialists Conference, pp: 1027-1032.

Ullah, N.R. and T. Thiringer, 2007. Variable speed wind turbines for power system stability enhancement. IEEE T. Energy Conver., 22: 52-60.

Vazquez, M.J.V., J.M.A. Marquez and F.S. Manzano, 2008. A methodology for optimizing stand-alone PV-system size using parallel-connected dc/dc converters. IEEE T. Ind. Electron., 55: 2664-2673.

Wai, R.J. and W.H. Wang, 2008. High-performance stand-alone photovoltaic generation system. IEEE T. Ind. Electron., 55: 240-250.

Yazdani, A. and R. Iravani, 2006. A neutral-point clamped converter system for direct-drive variable-speed wind power unit. IEEE T. Energy Conver., 21: 596-607.